
Model-Preserving Adaptive Rounding

Albert Tseng
 Cornell University
 albert@cs.cornell.edu

Zhaofeng Sun
 Cornell University
 zs453@cornell.edu

Christopher De Sa
 Cornell University
 cdesa@cs.cornell.edu

Abstract

The main goal of post-training quantization (PTQ) is to produce a compressed model whose output distribution is as close to the original model’s as possible. To do this tractably, almost all LLM PTQ algorithms quantize linear layers by independently minimizing the immediate activation error. However, this localized objective ignores the effect of subsequent layers, so reducing it does not necessarily give a closer model. In this work, we introduce Yet Another Quantization Algorithm (YAQA), an adaptive rounding algorithm that uses Kronecker-factored approximations of each linear layer’s Hessian with respect to the *full model* KL divergence. YAQA consists of two components: Kronecker-factored sketches of the full layerwise Hessian that can be tractably computed for hundred-billion parameter LLMs, and a quantizer-independent rounding algorithm that uses these sketches and comes with theoretical guarantees. Across a wide range of models and quantizers, YAQA empirically reduces the KL divergence to the original model by $\approx 30\%$ while achieving state of the art performance on downstream tasks.

1 Introduction

The ever-growing size of modern large language models (LLMs) continues to pose challenges for cost-effective and efficient deployment [22, 30]. One way to achieve better cost-benefit scaling is through quantization, which can greatly reduce the size and compute requirements of a model without significantly degrading quality [7]. For example, the latest post-training quantization (PTQ) methods can produce high quality 2-bit models, representing an $8\times$ size reduction over a 16-bit baseline [32, 20]. In memory-bound settings, this reduces I/O volume, and in compute-bound settings, using hardware-supported low precision datatypes can increase throughput [35].

At their core, PTQ methods, which quantize model parameters *after training*, can be viewed as generalized rounding algorithms that round high-precision model parameters θ^* to a set of representable low-precision points C . The goal of these methods is to minimize the distance between the original model outputs $M(\theta^*, X)$ and quantized model $M(\theta, X)$ over some inputs X sampled from an input distribution \mathcal{D} and model architecture M :

$$\hat{\theta} \leftarrow \arg \min_{\theta \in C} \mathbb{E}_{X \sim \mathcal{D}} D_{\text{KL}}(M(\theta^*, X) \| M(\theta, X)) \quad (1)$$

Here, we use the KL divergence between the model output distributions to measure how close two models are since the KL divergence is directly used in or closely related to core metrics in many downstream uses of quantized models [17, 25].

Unfortunately, exactly solving Equation 1 is intractable. While some works have proposed running constrained optimization on the full model KL, these methods do not consistently outperform quantization algorithms that use local second order information. Instead, virtually all state-of-the-art quantization algorithms such as LDLQ [3] and GPTQ [7] minimize the local layerwise activation error for each linear layer $W^* \in \mathbb{R}^{m \times n}$ as a proxy for Equation 1:

$$\arg \min_{W \in C} \mathbb{E}_{x \in \mathbb{R}^n \sim \mathcal{D}} \|x(W^* - W)^T\|_F^2 = \arg \min_{W \in C} \mathbb{E}_{x \sim \mathcal{D}} \text{tr}((W^* - W)x^T x(W^* - W)^T). \quad (2)$$

This de facto proxy objective admits a layerwise Hessian for the activation minimization problem $H_1 = \mathbb{E}_{x \sim \mathcal{D}}[x^T x]$, which is then used to quantize weights. However, since Equation 2 does not account for the effect of future layers on quantizing the current layer, quantizing with H_1 does not necessarily reduce Equation 1.

To remedy this, we introduce Yet Another Quantization Algorithm (YAQA), a new rounding algorithm that uses Kronecker-factored approximations of each linear layer’s Hessian with respect to the end-to-end KL divergence. Consider the second order expansion of the layerwise quantization problem at the original model for a linear layer $W^* \in \mathbb{R}^{m \times n}$:

$$\arg \min_{W \in C} \mathbb{E}_{X \sim \mathcal{D}} D_{\text{KL}}(M(\Theta^*, W^*, X) \| M(\Theta^*, W, X)) \approx \frac{1}{2}(W - W^*)^T (\nabla_{W^*}^2 L)(W - W^*) \quad (3)$$

where $L = D_{\text{KL}}(M(\Theta^*, W^*, X) \| M(\Theta^*, W, X))$, $\Theta^* = \theta^* \setminus W^*$ and first order terms involving $\nabla_{W^*} L$ are 0 since D_{KL} is minimized at the original model. Equation 3 is equivalent to assuming that the off-block diagonal elements of $\nabla_{\theta^*} L$ are 0, which recent works have suggested is empirically close to true [36]. Since the Hessian of the KL divergence is given by the Fisher Information Matrix, we can simplify $\nabla_{W^*}^2 L \in \mathbb{R}^{mn \times mn}$ to $\mathbb{E}[\text{vec}(\nabla_{W^*} \ell) \text{vec}(\nabla_{W^*} \ell)^T]$, where the expectation is taken over independent samples and ℓ is computed over the output distribution (see Section 3.1) [9]. Although $\nabla_{W^*}^2 L$ is too large to manifest, this structure lets us find Kronecker-factored approximations of $\nabla_{W^*}^2 L \approx (H_O \in \mathbb{R}^{m \times m}) \otimes (H_I \in \mathbb{R}^{n \times n})$ with Hessian-vector products.

These approximations form the basis of YAQA, which consists of two main components. First, we present a series of Hessian sketches that use Hessian-vector products to tractably compute close-to-optimal H_O, H_I for hundred billion parameter scale models. Then, we introduce a new adaptive rounding algorithm that can take advantage of these Hessians and comes with theoretical guarantees. This algorithm is quantizer independent, so YAQA can be used with hardware-supported datatypes (e.g. INT4) as well quantizers designed for memory-bound decoding (e.g. QTIP). Empirically, YAQA reduces the KL divergence by $\approx 30\%$ across a wide variety of models and quantizers while simultaneously achieving state of the art downstream task performance. In summary, we:

1. Introduce YAQA, which quantizes linear layers with Kronecker-factored approximations of the layerwise Hessian of the end-to-end KL divergence to the original model.
2. Describe close-to-optimal Kronecker-factored Hessian sketches that can be tractably computed for modern hundred-billion parameter LLMs.
3. Show that YAQA significantly reduces the KL divergence to the original model over existing rounding algorithms and achieves state of the art downstream results.

Our code to compute these Hessians and quantize models is available [here](#).

2 Background

2.1 Hessian Approximations

Prior works in optimization have proposed a wide variety Hessian sketches for modern neural networks. Most of these sketches are based off the Fisher Information Matrix $H = \mathbb{E}[\text{vec}(\nabla_{W^*} \ell) \text{vec}(\nabla_{W^*} \ell)^T]$, which is the Hessian of the KL divergence with respect to the parameters of a distribution [9]. In the “real” FIM, which corresponds to H , ℓ is computed with a Monte-Carlo sample over the model output logits, and in the “empirical” FIM, which is fundamentally different from H [16], ℓ is the task loss [21]. Since H is usually too large to manifest, past Hessian sketches have focused on producing Kronecker-factored approximations of $H \approx H_O \otimes H_I$.

In KFAC, the authors show that for linear layers in nonsequential models, $H = \mathbb{E}[x^T x \otimes (\nabla_y \ell)^T (\nabla_y \ell)]$ [21]. This gives a simple approximation of the real FIM: $H_I = \mathbb{E}[x^T x]$ and $H_O = \mathbb{E}[(\nabla_y \ell)^T (\nabla_y \ell)]$. In EKFAC, the authors add an eigencorrection to KFAC by observing that $\arg \min_{S \in \mathbb{R}^{mn}} \|H - (Q_O \otimes Q_I) \text{diag}(S)(Q_O \times Q_I)^T\|_F^2 = \mathbb{E}[Q_O^T (\nabla_{W^*} \ell) Q_I]$, where $Q_I S_I Q_I^T$ is the eigendecomposition of H_I and likewise for H_O [8]. Here, S corresponds to a better estimate of the eigenvalues of H vs. KFAC’s implicitly rank-1 eigenvalue approximation $S_O \otimes S_I$. In Shampoo and SOAP, the eigencorrected version of Shampoo, the authors propose approximating the *empirical* FIM with $H_I = \mathbb{E}[(\nabla_{W^*} \ell)^T (\nabla_{W^*} \ell)]$, $H_O = \mathbb{E}[(\nabla_{W^*} \ell)(\nabla_{W^*} \ell)^T]$, where $\nabla_{W^*} \ell$ is computed

batchwise [10, 34]. Finally, Adam corresponds to the eigencorrected approximation of the empirical Fisher using $H_I = H_O = I$ [15].

2.2 Model Compression

While PTQ has achieved popularity due to its combination of strong quality and relatively low resource overhead, there are many other ways of compressing models. For example, quantization aware training (QAT) and low precision training methods produce *natively quantized models* through modified training recipes [25, 33]. These methods require significantly more compute than PTQ but can give higher quality quantized models. In these settings, PTQ algorithms can be used for initialization or for rounding during training. Finally, methods such as pruning can also produce compressed models by removing entire parameters [12, 2, 29].

2.3 Layerwise Rounding and Incoherence Processing

Certain methods such as OBS, AdaRound, and SqueezeLLM have explored using information from the *empirical* Fisher matrix on the task loss (i.e., not the KL divergence to the original model) [12, 24, 14]. These methods assume the model is trained close to convergence and only use minimal information from the Empirical Fisher such as the diagonal. Such assumptions are not always true [13], which can lead to suboptimal performance. Furthermore, although quantizing models based on the empirical Fisher may reduce the task loss, the empirical Fisher is fundamentally different from the Hessian of the KL, so the resulting model may not be close to the original model [16]. In fact, the empirical Fisher of the KL is 0 since the KL is minimized at the original model and $\nabla_{W^*} \ell = 0$, so the empirical Fisher gives *no information* when with the KL.

Instead, most modern methods independently minimize the layerwise activation error with information from H_1 . In GPTQ and LDLQ, which are equivalent to each other, columns in W^* are iteratively rounded with linear feedback from the Cholesky decomposition of H_1 [3]. In AWQ, scaling from the activation channel norms is used to adjust the weights, corresponding to weighting the quantization problem by the diagonal of H_1 [18]. In QuIP, Chee et al. [3] showed that one could bound the proxy error $\text{tr}(\Delta W H_1 \Delta W^T)$ of LDLQ by an increasing function of H_1 's incoherence:

Definition 1 (Chee et al. [3]). *A Hessian $H \in \mathbb{R}^{n \times n}$ is μ -incoherent if its eigendecomposition $H = Q \Lambda Q^T$ has $\max_{i,j} |Q_{ij}| = \max_{i,j} |e_i^T Q e_j| \leq \mu/\sqrt{n}$.*

To reduce μ_{H_1} and thus the error of LDLQ, QuIP introduced *incoherence processing*, which conjugates H_1 and W^* by fast-to-multiply random orthogonal matrices $U \in \mathbb{R}^{m \times m}, V \in \mathbb{R}^{n \times n}$ to concentrate their entries: $\hat{W}^* \leftarrow UW^*V, \hat{H}_1 \leftarrow V^T H_1 V$. In QuIP#, Tseng et al. [31] improved QuIP's incoherence processing with the random Hadamard transform (RHT), which achieves, with probability $\geq 1 - \delta$, $\mu_H = \sqrt{2 \log(n^2/\delta)}$ and can be performed in $O(n \log n)$ time [11]. The RHT also makes W approximately i.i.d Gaussian, enabling the use of specially designed Gaussian quantizers [31, 32]. The RHT has since become widely adopted in PTQ and low precision training works [31–33, 1].

2.4 Finetuning and Gradient-Based Quantization

In Section 2.3, quantized representations are obtained without “learning” and are not updated once they are obtained. In contrast, certain recent methods have proposed finetuning algorithms that are essentially constrained QAT with a much smaller compute budget. In PV-Tuning, learnable codebooks and code point assignments are jointly optimized to minimize the end-to-end KL divergence [20]. In DiscQuant, model weights are updated with gradient descent on a constrained optimization problem over the full model KL divergence [4]. To the best of our knowledge, these two methods are the only prior quantization algorithms that explicitly consider the full model KL divergence over some localized proxy objective such as Equation 2.

3 Yet Another Quantization Algorithm

Here, we describe YAQA, a layerwise adaptive rounding method that rounds layers to minimize the full model KL divergence. YAQA consists of two components: 1) Kronecker-factored approximations

of the full layer Hessian with respect to the end-to-end KL divergence and 2) a theoretically principled rounding algorithm that uses these Kronecker-factored Hessians. With respect to the two “classes” of methods in Section 2, YAQA rounds layers in a one-shot way like methods in Section 2.3 but considers non-localized information like methods in Section 2.4. In the following sections, we first introduce two different Hessian sketches for close-to-optimal Kronecker-factored approximations of H that can be tractably computed for hundred billion parameter scale models. Then, we introduce our rounding algorithm that uses these Hessians and characterize its theoretical properties.

3.1 Kronecker Factored Hessians

Our goal is to find a H_I and H_O that can be tractably computed for modern hundred-billion parameter scale LLMs and $\nabla_{W^*}^2 L = H \approx H_O \otimes H_I$. Since the Kronecker product is a reshaped rank-1 product [19], a natural way to obtain H_I and H_O is to perform power iteration:

$$(H_I)_i \leftarrow \frac{H(H_O)_{i-1}}{\|(H_O)_{i-1}\|_F^2} \quad (H_O)_i \leftarrow \frac{(H_I)_{i-1}H}{\|(H_I)_{i-1}\|_F^2}. \quad (4)$$

However, obtaining a good estimate of H for power iteration is practically difficult. Recall that $H = \mathbb{E}[\text{vec}(\nabla_{W^*} \ell) \text{vec}(\nabla_{W^*} \ell)^T]$, where the expectation is taken over independent samples and ℓ is computed with a Monte-Carlo sampled target from the output logits z : $\ell = CE(t \sim \text{Cat}(z), z)$. In a LLM, tokens within a sequence are not independent due to sequence mixing from self-attention. As such, H must be computed over *entire sequences and not individual tokens*, which increases the variance of the estimate and makes increasing the sample size particularly expensive. Furthermore, to get a non rank-deficient estimate of $H_I \in \mathbb{R}^{n \times n}$, we need to backprop through $O(n)$ sequences (and likewise $O(m)$ for H_O). For large models where the intermediate dimension size is $O(10^4)$, this can be very expensive for multiple rounds of power iteration.

To remedy these issues, we propose two different Hessian sketches that both achieve strong empirical performance while being tractable to compute. Our first sketch (A) performs power iteration on a Hessian estimate that assumes tokens are independent within a linear layer. This lets us reduce the variance to $O(1/T)$, where T is the number of *tokens*, at the cost of a slightly biased estimate. Our second sketch (B) runs one round of power iteration on $\nabla_{W^*}^2 L$ starting from an identity matrix initialization, which we show can be computed in a single pass over a dataset. This lets us use enough sequences to achieve acceptable variance without making Hessian collection too expensive.

3.1.1 Hessian Sketch A

Sketch A performs power iteration on a Hessian estimate that assumes that attention does not mix within a sequence and tokens within a sequence are thus independent. In this setting,

$$(\nabla_{W^*}^2 L)_A = \mathbb{E}_{x \sim D} [x^T x \otimes (\nabla_y \ell)^T (\nabla_y \ell)] \quad (5)$$

where ℓ is computed with the same Monte-Carlo sample as before but each x, y pair corresponds to an *individual token*. This sketch is obviously biased but allows us to significantly reduce the variance by increasing the sample size to the number of tokens. Furthermore, $(\nabla_{W^*}^2 L)_A$ still has sequence information from $(\nabla_y \ell)$, so it is still empirically close to $\nabla_{W^*}^2 L$. To perform power iteration with $(\nabla_{W^*}^2 L)_A$, we compute

$$(H_I)_i \leftarrow \mathbb{E}_{x \sim D} [x^T x \langle (H_O)_{i-1}, (\nabla_y \ell)^T (\nabla_y \ell) \rangle] / \|(H_O)_{i-1}\|_F^2 \quad (6)$$

$$(H_O)_i \leftarrow \mathbb{E}_{x \sim D} [(\nabla_y \ell)^T (\nabla_y \ell) \langle (H_I)_{i-1}, x^T x \rangle] / \|(H_I)_{i-1}\|_F^2. \quad (7)$$

The only things required for Equation 6 are the input x and error signal $\frac{d\ell}{dy}$, so we can simply use a modified Pytorch backward pass that composes with FSDP to perform fully-distributed power iteration [26, 37]. To speed up convergence, we initialize $(H_I)_0 \leftarrow H_1 = \mathbb{E}[x^T x]$ and $(H_O)_0 \leftarrow I$. Empirically, power iteration converges in ≤ 3 full iterations with this initialization. End-to-end, sketch A takes around 30 GPU-hours for a $O(10B)$ parameter model and 20M token calibration set.

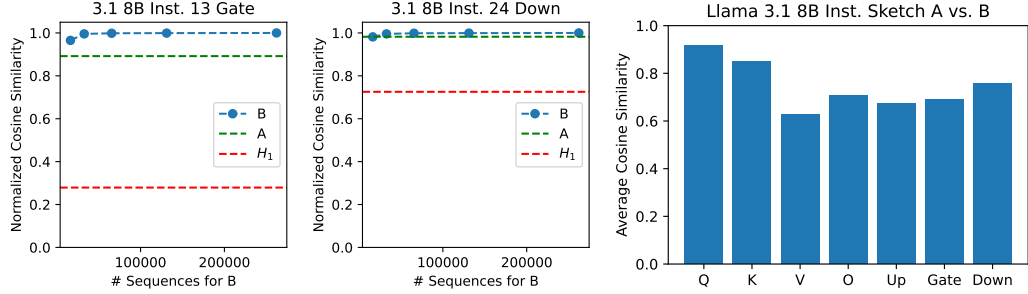


Figure 1: (L, C) Normalized cosine similarity of H_1 , A, and different sequence counts for B, calculated against 256K sequences. A and B are both significantly higher than H_1 . (R) Average actual cosine similarity between A and B over decoder layers by projection matrix. A and B are close to each other, with the pre-attention score layers showing higher similarity than other layers.

3.1.2 Hessian Sketch B

Sketch B directly computes the result of one round of power iteration on $\nabla_{W^*}^2 L$ starting with $H_I, H_O \leftarrow I$. Observe that power iterating on $\nabla_{W^*}^2 L$ involves computing the following updates

$$(H_I)_i \leftarrow \frac{\mathbb{E}_{s \sim D} [(\nabla_{W^*} \ell)^T (H_O)_{i-1} (\nabla_{W^*} \ell)]}{\|(H_O)_{i-1}\|_F^2} \quad (H_O)_i \leftarrow \frac{\mathbb{E}_{s \sim D} [(\nabla_{W^*} \ell) (H_I)_{i-1} (\nabla_{W^*} \ell)^T]}{\|(H_I)_{i-1}\|_F^2}. \quad (8)$$

If $(H_I)_0$ and $(H_O)_0$ are both I , then we have that $(H_I)_1 = \mathbb{E}_{s \sim D} [(\nabla_{W^*} \ell)^T (\nabla_{W^*} \ell)] / m$ and $(H_O)_1 = \mathbb{E}_{s \sim D} [(\nabla_{W^*} \ell) (\nabla_{W^*} \ell)^T] / n$ where the expectation and $\nabla_{W^*} \ell$ are computed over individual sequences. Both of these are easily computable in the same backward pass, letting us do one round of power iteration on both H_O and H_I in a *single pass over a dataset*. This sketch is conceptually similar to the preconditioning basis in Shampoo [10, 23], except that we compute the gradient per-sequence instead of per-batch and use the real Hessian instead of the empirical Fisher. End-to-end, sketch B takes around under 50 GPU-hours for a $O(10B)$ parameter model and 64K sequences of 2K tokens each.

3.1.3 Comparing Sketch A and Sketch B

Figure 1 Left and Center contain plots of the ‘‘normalized’’ cosine similarity of A, B computed with various dataset sizes, and $I \otimes H_1$, which corresponds to the layerwise activation error Hessian from Equation 2. computed against a ‘‘ground truth’’ H calculated with 256K sequences. Here, the normalized cosine similarity denotes $\frac{\langle H, H_O \otimes H_I \rangle}{\|H_O\| \|H_I\|}$, where H is calculated with 256K sequences and each plot is scaled so the largest data point is 1.0. This avoids computing $\|H\|$, which cannot be computed exactly in a tractable way and requires many expensive Hessian vector products to estimate with low variance. In general, the cosine similarities of A and B are both much higher than $I \otimes H_1$ and are close to each other, with A being slightly lower than B. In certain cases, such as for layer 24 Down in Llama 3.1 8B Instruct [22], A can actually have a higher cosine similarity than B estimated with a small dataset. This illustrates the case where the bias of A is less than the variance of B and where one might want to use A instead of B. Finally, Figure 1 Right shows that A and B have high cosine similarities $\frac{\langle (H_O)_A \otimes (H_I)_A, (H_O)_B \otimes (H_I)_B \rangle}{\|(H_O)_A\| \|(H_O)_B\| \|(H_I)_A\| \|(H_I)_B\|}$ to each other, with the pre-attention score layers (Q, K) having higher similarity than the post-attention score layers. This correlates with our construction of A, which assumes that attention does not do sequence mixing.

3.2 Adaptive Rounding with Kronecker Factored Hessians

Now, we describe a adaptive rounding algorithm that admits bounds on how well we can minimize Equation 3. Consider the family of adaptive rounding algorithms that rounds each entry as follows:

$$W_{i,j} = \mathcal{Q} (W^*_{i,j} + a_i^T (W^*_{:,j} - W_{:,j}) b_j + a_i^T (W^*_{:,j} - W_{:,j}) + (W^*_{i,:} - W_{i,:}) b_j), \quad (9)$$

where a_i is the i -th column of a strictly upper triangular $m \times m$ matrix L_O , b_j is the j -th column of a strictly upper triangular $n \times n$ matrix L_I , and \mathcal{Q} is a quantizer that performs nearest or stochastic

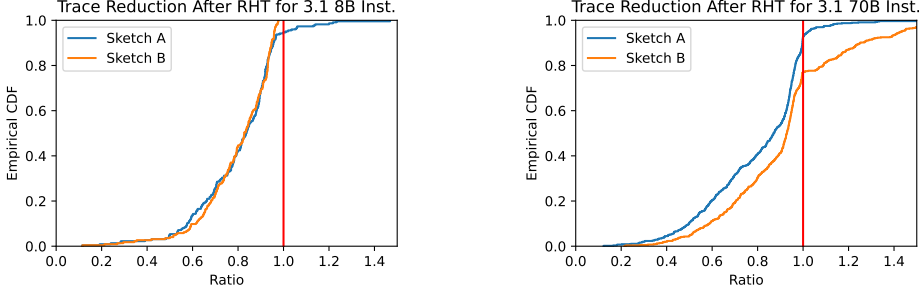


Figure 2: Empirical CDF of ratio of $\text{tr}(D_O^{\text{IP}}) \text{tr}(D_I^{\text{IP}})$ to $\text{tr}(D_O) \text{tr}(D_I)$, where D_I^{IP} denotes D_I after incoherence processing H_I with the RHT and likewise for D_O^{IP} and H_O . A ratio of < 1 (left of vertical red line) indicates a reduction in error bound. IP improves the error bound for most layers for both Hessian sketches.

rounding. Since L_O and L_I are both strictly triangular, the feedback in Equation 9 effectively comes from a rectangle “missing” a corner. For simplicity, we restrict our analysis to the scalar quantization case where each entry is rounded alone. The theory in this section translates to the vector quantization case, which we detail in the Appendix.

The final output of performing Equation 9 is a W that satisfies

$$W = \mathcal{Q}(W^* + L_O^T \Delta W L_I + L_O^T \Delta W + \Delta W L_I) \quad (10)$$

where $\Delta W = W^* - W$. If we choose L_O to be the LDL decomposition of H_O ($H_O = (L_O + I)D_O(L_O + I)^T$ for unit lower triangular L_O and diagonal D_O) and L_I to be the LDL decomposition of H_I ($H_I = (L_I + I)D_I(L_I + I)^T$) [27], then we can bound the error of the adaptive rounding procedure:

Theorem 1. Let $H_O \in \mathbb{R}^{m \times m}$ and $H_I \in \mathbb{R}^{n \times n}$ be two positive definite matrices and let \mathcal{Q} perform nearest or stochastic rounding with $\mathbb{E}[(\mathcal{Q}(x) - x)^2] \leq \sigma^2$. Furthermore, let W be the output of Equation 10 with L_O and L_I from the LDL decompositions of H_O and H_I , respectively. Then,

$$\Delta W (H_O \otimes H_I) \Delta W^T \leq \text{tr}(D_I) \text{tr}(D_O) \sigma^2 \leq \frac{\mu_I^2 \mu_O^2}{mn} \text{tr}(H_I^{1/2})^2 \text{tr}(H_O^{1/2})^2 \sigma^2$$

where $\Delta W = W^* - W$ and μ_O, μ_I are the incoherences of H_O, H_I (Definition 2).

Theorem 1 tells us that the error of YAQA is bounded by trace product $\text{tr}(D_O) \text{tr}(D_I)$, which can be correspondingly bounded by the incoherences of H_O and H_I . This suggests that like in LDLQ, we should reduce the incoherence of all Hessians before quantizing with incoherence processing. Figure 2 shows the empirical CDF across layers of the ratio $\frac{\text{tr}(D_O^{\text{IP}}) \text{tr}(D_I^{\text{IP}})}{\text{tr}(D_O) \text{tr}(D_I)}$, where D_I^{IP} denotes D_I after incoherence processing H_I with the RHT and likewise for D_O^{IP} and H_O . For the vast majority of layers in Llama 3.1 8B Instruct and 70B Instruct, incoherence processing reduces the trace bound.

Although H_O, H_I can be any positive definite matrices in Theorem 1, we can further bound the “true proxy error” $\Delta W H \Delta W^T$ – the thing we actually care about – with the cosine similarity between $H_O \otimes H_I$ and H :

Theorem 2. Let $H \in \mathbb{R}^{m \times n \times m \times n} = \nabla_{W*} L$ be the Hessian of a linear layer W with respect to the KL divergence to the original model outputs and let everything else be defined as in Theorem 1. Then,

$$\Delta W H \Delta W^T \leq \|H\| \left(\|\Delta W\|_F^2 \sqrt{2 - 2c} + \frac{\mu_I^2 \mu_O^2}{mn \|H_I\| \|H_O\|} \text{tr}(H_I^{1/2})^2 \text{tr}(H_O^{1/2})^2 \sigma^2 \right)$$

where $c = \frac{\langle H, H_O \otimes H_I \rangle}{\|H\| \|H_O\| \|H_I\|}$ is the cosine similarity between H and $H_O \otimes H_I$.

Theorem 2 lets us reason about when YAQA results in a tighter bound on the “true” layerwise proxy error than current state-of-the-art adaptive rounding methods LDLQ and equivalently GPTQ. First, observe that LDLQ is equivalent to running YAQA with $H_O \leftarrow I$ and $H_I \leftarrow H_I$. From Section 3.1.3 and Figure 1, we can empirically validate that c is much higher for both A and B than H_I . If we

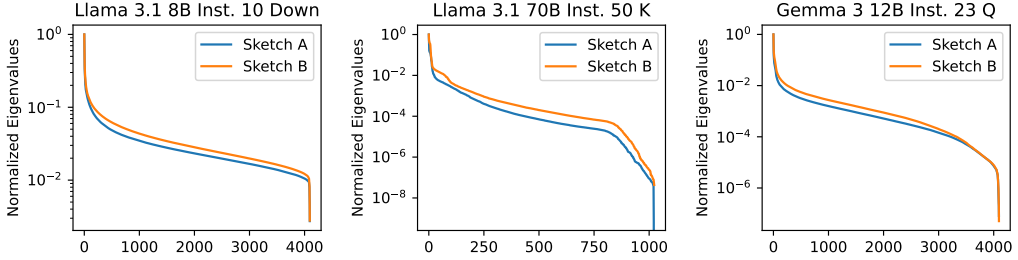


Figure 3: Real-world H_O ’s from A and B are approximately low rank and have similar spectrums.

assume that we have “reasonable” amounts of feedback and $\|\Delta W\|_F$ is approximately the same for both YAQA and LDLQ, which is empirically true, then $\|\Delta W\|_F \sqrt{2 - 2c}$ will be lower for YAQA.

Now, consider the part of Theorem 2 corresponding to the adaptive rounding incoherence bound from Theorem 1. In LDLQ, $H_O = I$ and $\text{tr}(D_O) = m$, so the ratio between the bound for arbitrary H_I and H_O and the bound for LDLQ is

$$\frac{\mu_O^2 \mu_I^2 \text{tr}(H_I^{1/2})^2 \|H_I\| \text{tr}(H_O^{1/2})^2}{m \sqrt{m} \mu_I^2 \text{tr}(H_I^{1/2})^2 \|H_I\| \|H_O\|}. \quad (11)$$

From Cauchy-Schwarz, $\text{tr}(H_O^{1/2})^2 \leq k_O \text{tr}(H_O)$, so if H_O has rank $k_O \leq \frac{m \mu_1^2 \text{tr}(H_1^{1/2})^2 \|H_I\|}{\mu_O^2 \mu_I^2 \text{tr}(H_I^{1/2})^2 \|H_1\|}$ then

Equation 11 $\leq \frac{\text{tr}(H_O)}{\sqrt{m} \|H_O\|} \leq 1$. This essentially tells us that when H_O is sufficiently low rank, the second term in Theorem 2 is smaller than the second term in Equation 11 and we should expect YAQA to better minimize the true proxy error $\Delta W H \Delta W^T$ than LDLQ. Indeed, Figure 3 shows that empirically, real-world H_O matrices have strong spectral decay and are approximately low rank.

4 Experiments

To test YAQA, we quantize Llama 3.1 and 3.2 Instruct models and evaluate both downstream perplexity and zeroshot accuracy and the KL divergence to the original model outputs (implementation details in Appendix). Although the KL divergence $D_{\text{KL}}(p||q) = \mathbb{E}_{x \sim p} \left[\log \frac{p(x)}{q(x)} \right]$ and perplexity $(-\log q(\tau)$ for a single target τ) are closely related, the KL divergence considers information outside of the target token τ whereas perplexity only considers the mass on τ . Thus, it is possible for two models to have the same perplexity but different D_{KL} ’s and vice versa, or even for a model to have higher perplexity but lower D_{KL} . Our goal is to produce a model as close to the original model as possible, so we consider a lower D_{KL} to indicate a closer model.

Baselines and Setup The focus of YAQA is on the Hessian estimate and rounding algorithm, so our main analysis is on “one-shot” quantization without any additional finetuning. However, we include experiments with recovery finetuning to show that YAQA composes with finetuning. For YAQA-A, we use a context length of 8K, ≈ 20 M tokens, and 3 full rounds of power iteration. For YAQA-B, we use a context length of 2K and 64K sequences. Our main rounding algorithm baseline is LDLQ, which is equivalent to the widely-used GPTQ and is the core rounding algorithm in many current state-of-the-art quantization works. We also include a smaller comparison to DiscQuant, which uses gradient-based optimization on the full-model KL. We do not directly compare to PV-Tuning since there are no public PV-Tuning models with either the QTIP or INT4 quantizer. However, LDLQ with the QTIP quantizer already outperforms PV-Tuning with the learnable AQLM quantizer on Llama 3.1, so we expect YAQA with QTIP to outperform PV-Tuning as well [32].

4.1 “One-Shot” Quantization

Table 1 shows our main results with the QTIP quantizer, incoherence processing, and no finetuning. Here, both YAQA Hessian sketches (YAQA-A and YAQA-B) consistently outperform LDLQ in KL divergence and downstream performance. YAQA-B generally outperforms YAQA-A due to its higher

Table 1: Results with incoherence processing, the QTIP quantizer, and no finetuning for Llama 3.1 and 3.2 Instruct models. YAQA strongly outperforms the LDLQ baseline that corresponds to the state-of-the-art QTIP paper, with YAQA-B outperforming YAQA-A due to being a better (but more expensive) Hessian estimate. Regardless, YAQA consistently reduces the KL divergence to the original model by a factor of $\approx 1/3$. Individual zeroshot results are in the Appendix.

ALGO.	BITS	$D_{KL} \downarrow$		$PPL \downarrow$		0-SHOT \uparrow		$D_{KL} \downarrow$		$PPL \downarrow$		0-SHOT \uparrow	
		W2		W2	C4	Avg		W2		W2	C4	Avg	
3.1 70B INST.													
BF16	16	0	3.52	6.46	67.67			0	9.58	10.62	63.79		
LDLQ	2	0.497	6.02	7.82	65.45			0.455	15.30	14.69	55.68		
	3	0.138	4.26	6.74	67.58			0.085	10.69	11.44	62.46		
	4	0.045	3.74	6.54	67.58			0.021	9.78	10.79	63.70		
YAQA-A	2	0.378	5.56	7.51	65.92			0.333	13.75	13.56	58.29		
	3	0.110	4.10	6.68	67.69			0.059	10.37	11.14	62.51		
	4	0.036	3.73	6.52	67.50			0.015	9.78	10.76	63.28		
YAQA-B	2	0.335	5.30	7.34	66.19			0.288	13.18	13.10	59.11		
	3	0.094	4.01	6.64	67.24			0.047	10.15	11.09	62.74		
	4	0.030	3.69	6.51	67.73			0.014	9.80	10.75	63.31		
3.1 8B INST.													
BF16	16	0	6.50	8.02	69.82			0	11.57	13.20	54.79		
LDLQ	2	0.356	9.39	10.70	62.51			0.527	19.86	19.66	49.60		
	3	0.069	7.05	8.50	69.29			0.109	12.95	14.44	52.89		
	4	0.019	6.63	8.15	69.41			0.032	12.05	13.63	53.47		
YAQA-A	2	0.284	8.79	10.09	64.06			0.371	17.22	17.64	50.02		
	3	0.050	6.89	8.38	69.09			0.072	12.56	14.02	53.86		
	4	0.015	6.62	8.13	69.62			0.021	11.83	13.44	54.17		
YAQA-B	2	0.241	8.39	9.83	64.32			0.334	16.66	17.36	50.90		
	3	0.044	6.85	8.34	69.31			0.065	12.51	13.97	53.41		
	4	0.013	6.61	8.12	69.78			0.019	11.83	13.41	53.84		
3.2 1B INST.													

Table 2: Results with incoherence processing, the INT4 quantizer, and no finetuning for Llama 3.1 8B Instruct. YAQA is quantizer agnostic and works with standard datatypes such as INT4.

ALGO.	$D_{KL} \downarrow$		$PPL \downarrow$		0-SHOT ACC \uparrow							
	W2		W2	C4	Avg	ARCC	ARCE	BOOLQ	HSWAG	PiQA		
BF16	0	6.50	8.02	69.82	51.37	78.03	82.05	57.74	79.92			
LDLQ	0.038	6.76	8.26	67.99	50.00	76.94	77.01	56.83	79.16			
DISCQUANT	0.061	6.83	8.37	67.68	50.34	77.44	74.12	56.55	79.92			
YAQA-A	0.028	6.71	8.21	69.11	50.68	78.11	79.65	57.13	79.98			
YAQA-B	0.029	6.72	8.23	68.92	49.49	77.31	81.01	56.98	79.82			

cosine similarity, at the cost of being more expensive to compute. Regardless, YAQA reduces the KL divergence to the original model by a factor of $\approx 1/3$ across all models and bitrates. Interestingly, all methods get similar perplexity at 4 bits but YAQA is still able to reduce the KL divergence, indicating that YAQA better preserves the output distribution outside of the target next token used to calculate perplexity. Table 2 shows results for quantizing Llama 3.1 8B Instruct with the INT4 quantizer without finetuning. Again, YAQA outperforms LDLQ in both KL divergence and downstream tasks. Table 2 also includes a comparison to DiscQuant. Interestingly, *LDLQ* also outperforms DiscQuant, showing that unlike YAQA, existing methods that optimize the end-to-end KL do not consistently outperform proxy objective-based methods.

4.2 How Much Does Finetuning Help?

Multiple recent PTQ works have included a “recovery finetuning” step that adjusts unquantized parameters to compensate for the effect of already-quantized parameters before quantization [6, 20,

Table 3: Results with the QTIP quantizer, incoherence processing, and recovery finetuning. Although recovery finetuning reduces the gap between YAQA and LDLQ, YAQA still improves upon LDLQ to achieve state-of-the-art results.

ALGO.	BITS	$D_{KL} \downarrow$		$PPL \downarrow$		0-SHOT \uparrow		$D_{KL} \downarrow$		$PPL \downarrow$		0-SHOT \uparrow	
		W2	W2	W2	C4	Avg	Avg	W2	W2	W2	C4	Avg	Avg
LLAMA 3.1 70B INSTRUCT												LLAMA 3.1 8B INSTRUCT	
BF16	16	0	3.52	6.46	67.67			0	6.50	8.02	69.82		
LDLQ	2	0.302	5.01	7.16	66.11			0.185	7.82	9.20	65.44		
	3	0.101	3.96	6.64	67.46			0.048	6.80	8.31	68.42		
	4	0.036	3.71	6.54	67.64			0.016	6.61	8.13	69.47		
	2	0.279	4.92	7.10	66.26			0.163	7.63	9.06	67.54		
YAQA-A	3	0.098	3.88	6.63	66.94			0.042	6.78	8.28	69.23		
	4	0.032	3.68	6.52	67.59			0.014	6.58	8.10	69.50		
	2	0.266	4.82	7.07	66.99			0.147	7.60	8.96	66.38		
YAQA-B	3	0.091	3.87	6.61	67.42			0.038	6.74	8.27	68.88		
	4	0.029	3.67	6.52	67.69			0.012	6.56	8.11	70.12		

Table 4: Results for Gemma 3 12B Inst. with INT4 *without finetuning*. Despite being trained on the original model’s outputs, the QAT model has a higher D_{KL} to the original model than the YAQA models. The QAT model also somehow outperforms the original model in downstream evals, implying that the QAT process is producing a considerably different model.

ALGO.	QUANT. TYPE	BITS	$D_{KL} \downarrow$		$PPL \downarrow$		0-SHOT ACC \uparrow					
			W2	W2	W2	C4	Avg	ARCC	ARCE	BOOLQ	HSWAG	PIQA
BF16	NONE	16	0	7.85	8.61	70.22	54.01	78.79	87.25	54.27	76.77	
GOOGLE QAT	QAT	4.5	0.089	7.56	8.52	70.83	54.52	79.76	86.82	54.77	78.29	
YAQA-A	PTQ	4	0.058	7.96	8.69	70.12	53.90	78.83	87.09	53.68	77.09	
YAQA-B	PTQ	4	0.056	7.94	8.67	69.90	54.10	78.66	86.91	54.13	75.68	

31, 32]. While recovery finetuning methods are mostly ad-hoc, their main goal is still to preserve the original model. This raises the question: how much of YAQA’s improvements over LDLQ can be recovered from finetuning? Table 3 shows an experiment with QuIP#’s recovery finetuning algorithm (details in Appendix) on top of the setup in 1 [31]. This finetuning algorithm was developed and optimized for LDLQ, so it is entirely possible that a better finetuning algorithm exists for YAQA, which we leave for future work. For both models, recovery finetuning reduces the gap between LDLQ and YAQA. However, YAQA still reduces the KL divergence to the original model by $\approx 10\text{-}20\%$ and maintains a gap in downstream tasks, suggesting that YAQA uses global information that is not available during recovery finetuning. Finally, we note that the LDLQ results in this table correspond to the results in the state-of-the-art QTIP paper, so YAQA’s results Table 3 set a new state of the art across all PTQ methods and quantizers.

4.3 How Does YAQA Compare to Quantization Aware Training?

While YAQA is a PTQ method, it is perhaps interesting to compare it to much more expensive QAT methods that also try to preserve the original model. Table 4 compares YAQA with INT4 and no finetuning against Google’s official QAT version of Gemma 3 12B Instruct, which uses a 4.5 bit datatype [30]. We estimate the QAT process took $O(10^9)$ tokens, or $100\times$ more data than YAQA. Although the QAT model somehow outperforms the original model in downstream tasks despite being trained on the original model outputs [30], YAQA models have a lower KL divergence to the original model. YAQA also maintains a smaller gap in downstream performance, suggesting that the QAT process is actually producing a considerably different model from the original model.

5 Conclusion

In this work, we present YAQA, a new LLM PTQ algorithm that quantizes linear layers with Kronecker-factored approximations of the Hessian with respect to the full model KL divergence. By considering the end-to-end KL divergence, YAQA improves upon existing state-of-the-art PTQ methods – the vast majority of which only consider local layerwise activation errors. YAQA consists of two parts: near-optimal Kronecker-factored Hessian sketches for the full-model KL that can be tractably computed for hundred-billion parameter scale models, and a new adaptive rounding algorithm for these Hessians that comes with theoretical guarantees. Empirically, YAQA reduces the KL divergence to the original model by $\approx 30\%$ over LDLQ and GPTQ, setting a new benchmark in post training quantization performance.

Acknowledgments

A.T. was supported by the NSF Graduate Research Fellowship. C.D. was supported by DARPA D24AP00259-00. We thank Together AI for compute resources.

References

- [1] Saleh Ashkboos, Amirkeivan Mohtashami, Maximilian L. Croci, Bo Li, Martin Jaggi, Dan Alistarh, Torsten Hoefer, and James Hensman. Quarot: Outlier-free 4-bit inference in rotated llms, 2024.
- [2] Jerry Chee, Megan Renz, Anil Damle, and Christopher De Sa. Model preserving compression for neural networks. In Alice H. Oh, Alekh Agarwal, Danielle Belgrave, and Kyunghyun Cho, editors, *Advances in Neural Information Processing Systems*, 2022. URL <https://openreview.net/forum?id=gt-19Hu2ndd>.
- [3] Jerry Chee, Yaohui Cai, Volodymyr Kuleshov, and Christopher De Sa. QuIP: 2-bit quantization of large language models with guarantees. In *Thirty-seventh Conference on Neural Information Processing Systems*, 2023. URL <https://openreview.net/forum?id=xrk9g5vcXR>.
- [4] Jerry Chee, Arturs Backurs, Rainie Heck, Li Zhang, Janardhan Kulkarni, Thomas Rothvoss, and Sivakanth Gopi. Discquant: A quantization method for neural networks inspired by discrepancy theory, 2025. URL <https://arxiv.org/abs/2501.06417>.
- [5] Together Computer. Redpajama: An open source recipe to reproduce llama training dataset, 2023. URL <https://github.com/togethercomputer/RedPajama-Data>.
- [6] Vage Egiazarian, Andrei Panferov, Denis Kuznedelev, Elias Frantar, Artem Babenko, and Dan Alistarh. Extreme compression of large language models via additive quantization, 2024.
- [7] Elias Frantar, Saleh Ashkboos, Torsten Hoefer, and Dan Alistarh. OPTQ: Accurate quantization for generative pre-trained transformers. In *The Eleventh International Conference on Learning Representations*, 2023. URL <https://openreview.net/forum?id=tcbBPnfwxS>.
- [8] Thomas George, César Laurent, Xavier Bouthillier, Nicolas Ballas, and Pascal Vincent. Fast approximate natural gradient descent in a kronecker factored eigenbasis. In S. Bengio, H. Wallach, H. Larochelle, K. Grauman, N. Cesa-Bianchi, and R. Garnett, editors, *Advances in Neural Information Processing Systems*, volume 31. Curran Associates, Inc., 2018. URL https://proceedings.neurips.cc/paper_files/paper/2018/file/48000647b315f6f00f913caa757a70b3-Paper.pdf.
- [9] Christian Gourieroux and Alain Monfort. *Statistics and Econometric Models*. Number 9780521471626 in Cambridge Books. Cambridge University Press, December 1995. URL <https://ideas.repec.org/b/cup/cbooks/9780521471626.html>.
- [10] Vineet Gupta, Tomer Koren, and Yoram Singer. Shampoo: Preconditioned stochastic tensor optimization. In Jennifer Dy and Andreas Krause, editors, *Proceedings of the 35th International Conference on Machine Learning*, volume 80 of *Proceedings of Machine Learning Research*, pages 1842–1850. PMLR, 10–15 Jul 2018. URL <https://proceedings.mlr.press/v80/gupta18a.html>.
- [11] Nathan Halko, Per-Gunnar Martinsson, and Joel A Tropp. Finding structure with randomness: Probabilistic algorithms for constructing approximate matrix decompositions. *SIAM review*, 53(2):217–288, 2011.
- [12] Babak Hassibi, David Stork, and Gregory Wolff. Optimal brain surgeon: Extensions and performance comparisons. In J. Cowan, G. Tesauro, and J. Alspector, editors, *Advances in Neural Information Processing Systems*, volume 6. Morgan-Kaufmann, 1993. URL https://proceedings.neurips.cc/paper_files/paper/1993/file/b056eb1587586b71e2da9acfe4fbd19e-Paper.pdf.
- [13] Jordan Hoffmann, Sebastian Borgeaud, Arthur Mensch, Elena Buchatskaya, Trevor Cai, Eliza Rutherford, Diego de Las Casas, Lisa Anne Hendricks, Johannes Welbl, Aidan Clark, Tom Hennigan, Eric Noland, Katie Millican, George van den Driessche, Bogdan Damoc, Aurelia Guy, Simon Osindero, Karen Simonyan, Erich Elsen, Jack W. Rae, Oriol Vinyals, and Laurent Sifre. Training compute-optimal large language models, 2022. URL <https://arxiv.org/abs/2203.15556>.

[14] Sehoon Kim, Coleman Hooper, Amir Gholami, Zhen Dong, Xiuyu Li, Sheng Shen, Michael Mahoney, and Kurt Keutzer. Squeezellm: Dense-and-sparse quantization. *arXiv*, 2023.

[15] Diederik P. Kingma and Jimmy Ba. Adam: A method for stochastic optimization, 2017.

[16] Frederik Kunstner, Lukas Balles, and Philipp Hennig. Limitations of the empirical fisher approximation for natural gradient descent, 2020. URL <https://arxiv.org/abs/1905.12558>.

[17] Yaniv Leviathan, Matan Kalman, and Yossi Matias. Fast inference from transformers via speculative decoding. In Andreas Krause, Emma Brunskill, Kyunghyun Cho, Barbara Engelhardt, Sivan Sabato, and Jonathan Scarlett, editors, *Proceedings of the 40th International Conference on Machine Learning*, volume 202 of *Proceedings of Machine Learning Research*, pages 19274–19286. PMLR, 23–29 Jul 2023. URL <https://proceedings.mlr.press/v202/leviathan23a.html>.

[18] Ji Lin, Jiaming Tang, Haotian Tang, Shang Yang, Xingyu Dang, Chuang Gan, and Song Han. Awq: Activation-aware weight quantization for llm compression and acceleration, 2023.

[19] Charles F. Van Loan. The ubiquitous kronecker product. *Journal of Computational and Applied Mathematics*, 123(1):85–100, 2000. ISSN 0377-0427. doi: [https://doi.org/10.1016/S0377-0427\(00\)00393-9](https://doi.org/10.1016/S0377-0427(00)00393-9). URL <https://www.sciencedirect.com/science/article/pii/S0377042700003939>. Numerical Analysis 2000. Vol. III: Linear Algebra.

[20] Vladimir Malinovskii, Denis Mazur, Ivan Ilin, Denis Kuznedelev, Konstantin Pavlovich Burlachenko, Kai Yi, Dan Alistarh, and Peter Richtárik. PV-tuning: Beyond straight-through estimation for extreme LLM compression. In *The Thirty-eighth Annual Conference on Neural Information Processing Systems*, 2024. URL <https://openreview.net/forum?id=YvA8UF0I37>.

[21] James Martens and Roger Grosse. Optimizing neural networks with kronecker-factored approximate curvature. In Francis Bach and David Blei, editors, *Proceedings of the 32nd International Conference on Machine Learning*, volume 37 of *Proceedings of Machine Learning Research*, pages 2408–2417, Lille, France, 07–09 Jul 2015. PMLR. URL <https://proceedings.mlr.press/v37/martens15.html>.

[22] meta llama. llama3. <https://github.com/meta-llama/llama3>, 2024.

[23] Depen Morwani, Itai Shapira, Nikhil Vyas, eran malach, Sham M. Kakade, and Lucas Janson. A new perspective on shampoo’s preconditioner. In *The Thirteenth International Conference on Learning Representations*, 2025. URL <https://openreview.net/forum?id=c6zI3Cp8c6>.

[24] Markus Nagel, Rana Ali Amjad, Mart Van Baalen, Christos Louizos, and Tijmen Blankevoort. Up or down? Adaptive rounding for post-training quantization. In Hal Daumé III and Aarti Singh, editors, *Proceedings of the 37th International Conference on Machine Learning*, volume 119 of *Proceedings of Machine Learning Research*, pages 7197–7206. PMLR, 13–18 Jul 2020. URL <https://proceedings.mlr.press/v119/nagel20a.html>.

[25] Markus Nagel, Marios Fournarakis, Yelysei Bondarenko, and Tijmen Blankevoort. Overcoming oscillations in quantization-aware training. In Kamalika Chaudhuri, Stefanie Jegelka, Le Song, Csaba Szepesvari, Gang Niu, and Sivan Sabato, editors, *Proceedings of the 39th International Conference on Machine Learning*, volume 162 of *Proceedings of Machine Learning Research*, pages 16318–16330. PMLR, 17–23 Jul 2022. URL <https://proceedings.mlr.press/v162/nagel22a.html>.

[26] Adam Paszke, Sam Gross, Francisco Massa, Adam Lerer, James Bradbury, Gregory Chanan, Trevor Killeen, Zeming Lin, Natalia Gimelshein, Luca Antiga, Alban Desmaison, Andreas Köpf, Edward Yang, Zach DeVito, Martin Raison, Alykhan Tejani, Sasank Chilamkurthy, Benoit Steiner, Lu Fang, Junjie Bai, and Soumith Chintala. Pytorch: An imperative style, high-performance deep learning library, 2019. URL <https://arxiv.org/abs/1912.01703>.

[27] K. B. Petersen and M. S. Pedersen. The matrix cookbook, nov 2012. URL <http://www2.compute.dtu.dk/pubdb/pubs/3274-full.html>. Version 20121115.

[28] Neil Sloane. Hadamard Matrices — neilsloane.com. <http://neilsloane.com/hadamard/>. [Accessed 02-02-2024].

[29] Mingjie Sun, Zhuang Liu, Anna Bair, and J Zico Kolter. A simple and effective pruning approach for large language models. In *Workshop on Efficient Systems for Foundation Models @ ICML2023*, 2023. URL <https://openreview.net/forum?id=tz9JV2PRSV>.

[30] Gemma Team, Aishwarya Kamath, Johan Ferret, Shreya Pathak, Nino Vieillard, Ramona Merhej, Sarah Perrin, Tatiana Matejovicova, Alexandre Ramé, Morgane Rivière, Louis Rouillard, Thomas Mesnard, Geoffrey Cideron, Jean bastien Grill, Sabela Ramos, Edouard Yvinec, Michelle Casbon, Etienne Pot, Ivo Penchev, Gaël Liu, Francesco Visin, Kathleen Kenealy, Lucas Beyer, Xiaohai Zhai, Anton Tsitsulin, Robert Busa-Fekete, Alex Feng, Noveen Sachdeva, Benjamin Coleman, Yi Gao, Basil Mustafa, Iain Barr, Emilio Parisotto, David Tian, Matan Eyal, Colin Cherry, Jan-Thorsten Peter, Danila Sinopalnikov, Surya Bhupatiraju, Rishabh Agarwal, Mehran Kazemi, Dan Malkin, Ravin Kumar, David Vilar, Idan Brusilovsky, Jiaming Luo, Andreas Steiner, Abe Friesen, Abhanshu Sharma, Abheesht Sharma, Adi Mayrav Gilady, Adrian Goedeckemeyer, Alaa Saade, Alex Feng, Alexander Kolesnikov, Alexei Bendebury, Alvin Abdagic, Amit Vadi, András György, André Susano Pinto, Anil Das, Ankur Bapna, Antoine Miech, Antoine Yang, Antonia Paterson, Ashish Shenoy, Ayan Chakrabarti, Bilal Piot, Bo Wu, Bobak Shahriari, Bryce Petrini, Charlie Chen, Charlène Le Lan, Christopher A. Choquette-Choo, CJ Carey, Cormac Brick, Daniel Deutsch, Danielle Eisenbud, Dee Cattle, Derek Cheng, Dimitris Paparas, Divyashree Shivakumar Sreepathihalli, Doug Reid, Dustin Tran, Dustin Zelle, Eric Noland, Erwin Huizenga, Eugene Kharitonov, Frederick Liu, Gagik Amirkhanyan, Glenn Cameron, Hadi Hashemi, Hanna Klimczak-Plucińska, Harman Singh, Harsh Mehta, Harshal Tushar Lehri, Hussein Hazimeh, Ian Ballantyne, Idan Szpektor, Ivan Nardini, Jean Pouget-Abadie, Jetha Chan, Joe Stanton, John Wieting, Jonathan Lai, Jordi Orbay, Joseph Fernandez, Josh Newlan, Ju yeong Ji, Jyotinder Singh, Kat Black, Kathy Yu, Kevin Hui, Kiran Vodrahalli, Klaus Greff, Linhai Qiu, Marcella Valentine, Marina Coelho, Marvin Ritter, Matt Hoffman, Matthew Watson, Mayank Chaturvedi, Michael Moynihan, Min Ma, Nabila Babar, Natasha Noy, Nathan Byrd, Nick Roy, Nikola Momchev, Nilay Chauhan, Noveen Sachdeva, Oskar Bunyan, Pankil Botarda, Paul Caron, Paul Kishan Rubenstein, Phil Culliton, Philipp Schmid, Pier Giuseppe Sessa, Pingmei Xu, Piotr Stanczyk, Pouya Tafti, Rakesh Shivanna, Renjie Wu, Renke Pan, Reza Rokni, Rob Willoughby, Rohith Vallu, Ryan Mullins, Sammy Jerome, Sara Smoot, Sertan Girgin, Shariq Iqbal, Shashir Reddy, Shruti Sheth, Siim Põder, Sijal Bhatnagar, Sindhu Raguram Panyam, Sivan Eiger, Susan Zhang, Tianqi Liu, Trevor Yacovone, Tyler Liechty, Uday Kalra, Utku Evci, Vedant Misra, Vincent Roseberry, Vlad Feinberg, Vlad Kolesnikov, Woohyun Han, Woosuk Kwon, Xi Chen, Yinlam Chow, Yuvein Zhu, Zichuan Wei, Zoltan Egyed, Victor Cotruta, Minh Giang, Phoebe Kirk, Anand Rao, Kat Black, Nabila Babar, Jessica Lo, Erica Moreira, Luiz Gustavo Martins, Omar Sanseviero, Lucas Gonzalez, Zach Gleicher, Tris Warkentin, Vahab Mirrokni, Evan Senter, Eli Collins, Joelle Barral, Zoubin Ghahramani, Raia Hadsell, Yossi Matias, D. Sculley, Slav Petrov, Noah Fiedel, Noam Shazeer, Oriol Vinyals, Jeff Dean, Demis Hassabis, Koray Kavukcuoglu, Clement Farabet, Elena Buchatskaya, Jean-Baptiste Alayrac, Rohan Anil, Dmitry, Lepikhin, Sebastian Borgeaud, Olivier Bachem, Armand Joulin, Alek Andreev, Cassidy Hardin, Robert Dadashi, and Léonard Hussenot. Gemma 3 technical report, 2025. URL <https://arxiv.org/abs/2503.19786>.

[31] Albert Tseng, Jerry Chee, Qingyao Sun, Volodymyr Kuleshov, and Christopher De Sa. Quip#: Even better l1m quantization with hadamard incoherence and lattice codebooks, 2024.

[32] Albert Tseng, Qingyao Sun, David Hou, and Christopher De Sa. QTIP: Quantization with trellises and incoherence processing. In *The Thirty-eighth Annual Conference on Neural Information Processing Systems*, 2024. URL <https://openreview.net/forum?id=7sdkLVuYCU>.

[33] Albert Tseng, Tao Yu, and Youngsuk Park. Training LLMs with MXFP4. In *The 28th International Conference on Artificial Intelligence and Statistics*, 2025. URL <https://openreview.net/forum?id=a8z5Q0WSPL>.

[34] Nikhil Vyas, Depen Morwani, Rosie Zhao, Itai Shapira, David Brandfonbrener, Lucas Janson, and Sham M. Kakade. SOAP: Improving and stabilizing shampoo using adam for language modeling. In *The Thirteenth International Conference on Learning Representations*, 2025. URL <https://openreview.net/forum?id=IDxZhXrpNf>.

- [35] Charlene Yang, Yunsong Wang, Steven Farrell, Thorsten Kurth, and Samuel Williams. Hierarchical roofline performance analysis for deep learning applications, 2020. URL <https://arxiv.org/abs/2009.05257>.
- [36] Yushun Zhang, Congliang Chen, Ziniu Li, Tian Ding, Chenwei Wu, Diederik P Kingma, Yinyu Ye, Zhi-Quan Luo, and Ruoyu Sun. Adam-mini: Use fewer learning rates to gain more. In *The Thirteenth International Conference on Learning Representations*, 2025. URL <https://openreview.net/forum?id=iBExhaU3Lc>.
- [37] Yanli Zhao, Andrew Gu, Rohan Varma, Liang Luo, Chien-Chin Huang, Min Xu, Less Wright, Hamid Shojanazeri, Myle Ott, Sam Shleifer, Alban Desmaison, Can Balioglu, Pritam Damania, Bernard Nguyen, Geeta Chauhan, Yuchen Hao, Ajit Mathews, and Shen Li. Pytorch fsdp: Experiences on scaling fully sharded data parallel, 2023. URL <https://arxiv.org/abs/2304.11277>.

A Appendix

A.1 Experimental Setup and Implementation Details

All Hessians were collected using the RedPajama v1 dataset [5]. We use Hadamard matrices from Neil Sloane’s website for the “base Hadamard matrix” in incoherence processing as described in Section A.3 [28]. We use the OPTQ “Wikitext2” and “C4” dataset splits for KL divergence and perplexity calculation [7]. We use a sequence length of 8192 for all KL divergence and perplexity evaluations. We evaluate all zero-shot results with the chat template applied. For finetuning experiments, we use the same setup as QTIP except that we normalize the activation error due to numerical instability from the default Adam $\epsilon = 10^{-8}$. For all Llama 3.1 70B Instruct experiments, we do not quantize the 0_v layer. The Gemma QAT comparison was run with the `google/gemma-3-12b-it-qat-q4_0-gguf` model on Huggingface, which was dequantized with the 4.52.0.dev0 nightly version of Transformers. Our code will be available on Github at a later date.

A.2 Memory and Compute Requirements

YQAQ requires storing $O(n^2)$ memory for H_I and $O(m^2)$ memory for H_O . In practice, we only need to store the lower triangular parts of H_I and H_O since they are symmetric. LDLQ and other layerwise activation methods only need to store H_I , so YQAQ requires roughly double the storage for the Hessians. We found that computing and storing the Hessians in FP32 was sufficient to maintain numerical stability and positive-definiteness with a small regularization factor on the diagonal ($\approx 10^{-4} \text{tr}(H)/n$), but using TF32 for computations was not. The computational cost of computing Hessians with Sketch B is $O(btmn + bn^2m + bm^2n)$ on top of the cost of a forward pass and backprop, where b is the number of sequences and t is the average number of tokens per sequence. The computational cost of computing Hessians with Sketch A is $O(pbt(n^2 + m^2))$, again on top of a forward pass and backward pass, where p is the number of steps of power iteration. Since we must use a larger b for Sketch B than Sketch A to get acceptable variance, Sketch B is empirically slower than Sketch A.

A.3 Incoherence Processing with the Random Hadamard Transform

Although we describe incoherence processing for Hessians in the main body, incoherence processing also modifies the weights. The full definition of incoherence, including *weight incoherence*, is as follows:

Definition 2 (Chee et al. [3]). *A Hessian $H \in \mathbb{R}^{n \times n}$ is μ -incoherent if its eigendecomposition $H = Q\Lambda Q^T$ has $\max_{i,j} |Q_{ij}| = \max_{i,j} |e_i^T Q e_j| \leq \mu/\sqrt{n}$. A weight matrix $W \in \mathbb{R}^{m \times n}$ is μ -incoherent if $\max_{i,j} |W_{ij}| = \max_{i,j} |e_i^T W e_j| \leq \mu\|W\|_F/\sqrt{mn}$.*

Incoherence processing with the RHT applies a Random Hadamard Transformation on W and H . Let H be a Hadamard matrix, defined as follows:

$$H_1 = [1] \quad H_n = \frac{1}{2} \begin{bmatrix} H_{n-1} & H_{n-1} \\ H_{n-1} & -H_{n-1} \end{bmatrix} \quad (12)$$

Then, the RHT performs $x \leftarrow H_{\log_2 n} S x$, where S is a random sign vector $\in \{\pm 1\}^n$, $x \in \mathbb{R}^n$, and n is a power of 2. For non power-of-2 n , we follow QuIP# and use a fixed “small” Hadamard matrix as a base instead of H_1 . Full proofs for bounds on the behavior of the RHT can be found in QuIP#.

A.4 YQAQ Rounding Algorithm

The YQAQ rounding algorithm can be written as a fixed point iteration (Algorithm 1). It can also be implemented iteratively (Python code), which is faster for slower quantizers than the fixed point iteration implementation above.

Algorithm 1 YAQA Rounding Algorithm Fixed Point Iteration

Require: Weight matrix $W \in \mathbb{R}^{m \times n}$, p.d. $H_O \in \mathbb{R}^{m \times m}$, p.d. $H_I \in \mathbb{R}^{n \times n}$, quantizer \mathcal{Q} , quantizer block sizes $g_x \in \mathbb{Z}^+ | m, g_y \in \mathbb{Z}^+ | n$.

- 1: $L_O, D_O \leftarrow \text{BlockLDL}(H_O, g_x)$
- 2: $L_I, D_I \leftarrow \text{BlockLDL}(H_I, g_y)$
- 3: $\hat{W} \leftarrow \mathcal{Q}(W)$
- 4: $\text{converged} \leftarrow \text{false}$
- 5: $\hat{W}^* \leftarrow \hat{W}$
- 6: **while** not converged **do**
- 7: $\Delta W \leftarrow W - \hat{W}$
- 8: $\hat{W} = \mathcal{Q}(W + L_O^T \Delta W L_I + L_O^T \Delta W + \Delta W L_I)$
- 9: $\text{converged} \leftarrow (\hat{W} == \hat{W}^*)$
- 10: $\hat{W}^* \leftarrow \hat{W}$
- 11: **end while**
- 12: **return** Quantized \hat{W} .

```

def YAQA_iterative(W, Lin, Lout, td_x, td_y, cb):
    m, n = W.shape
    hatW = torch.zeros_like(W)
    Qidxs = torch.zeros(m, n, dtype=cb.idx_dtype, device=W.device)
    assert m % td_x == 0 and n % td_y == 0
    starts = [[(m//td_x-i-1, n//td_y-i-1) for i in range(m//td_x)], [(0, n//td_y-i-1) for i in range(n//td_y)]]

    for i in tqdm(range(m//td_x + n//td_y)):
        target = []
        target_idx = []
        start = starts[i]
        jmax = max(start[0], start[1])
        jm, jn = start
        while 0 <= jm < m//td_x and 0 <= jn < n//td_y:
            thing = W[jm*td_x:(jm+1)*td_x, jn*td_y:(jn+1)*td_y] + (Lout[jm*td_x:, jm*td_x:(jm+1)*td_x] *
            T @ (W[jm*td_x:, jn*td_y:] - hatW[jm*td_x:, jn*td_y:]) @ Lin[jn*td_y:, jn*td_y:(jn+1)*td_y] + Lout
            [jm*td_x:, jm*td_x:(jm+1)*td_x].T @ (W[jm*td_x:, jn*td_y:(jn+1)*td_y] - hatW[jm*td_x:, jn*td_y:(jn+1)*td_y]) +
            (W[jm*td_x:(jm+1)*td_x, jn*td_y:] - hatW[jm*td_x:(jm+1)*td_x, jn*td_y:]) @ Lin[jn*td_y:, jn*td_y:(jn+1)*td_y])
            target.append(thing)
            target_idx.append((jm, jn))
            jm += 1
            jn -= 1

        target = torch.stack(target, dim=0).reshape(-1, td_x * td_y)
        qtarget, target_idx = cb.quantize(target)
        qtarget = qtarget.reshape(-1, td_x, td_y)
        target_idx = target_idx.reshape(-1, td_x, td_y)

        for j in range(len(target_idx)):
            jm, jn = target_idx[j]
            hatW[jm*td_x:(jm+1)*td_x, jn*td_y:(jn+1)*td_y] = qtarget[j]
            Qidxs[jm*td_x:(jm+1)*td_x, jn*td_y:(jn+1)*td_y] = target_idx[j]

    return hatW, Qidxs

```

A.5 Proofs

Theorem 3. Let $H_O \in \mathbb{R}^{m \times m}$ and $H_I \in \mathbb{R}^{n \times n}$ be two positive definite matrices and let \mathcal{Q} perform nearest or stochastic rounding independently on blocks of $g_x \times g_y$ with $\mathbb{E}[(\mathcal{Q}(\text{vec}(x)) - \text{vec}(x))(\mathcal{Q}(\text{vec}(x)) - \text{vec}(x))^T] \preceq \sigma^2 I$. Furthermore, let W be the output of Equation 10 with L_O and L_I from the g_x and g_y -block LDL decompositions of H_O and H_I , respectively. Then,

$$\Delta W (H_O \otimes H_I) \Delta W^T \leq \text{tr}(D_I) \text{tr}(D_O) g_x g_y \sigma^2 \leq \frac{g_x g_y \mu_I^2 \mu_O^2}{mn} \text{tr}(H_I^{1/2})^2 \text{tr}(H_O^{1/2})^2 \sigma^2$$

where $\Delta W = W^* - W$ and μ_O, μ_I are the incoherences of H_O, H_I (Definition 2).

Proof. Let

$$\eta = W^* + L_O^T \Delta W L_I + L_O^T \Delta W + \Delta W L_I - W \quad (13)$$

$$= (L_O + I)^T \Delta W (L_I + I) \quad (14)$$

Then,

$$\Delta W(H_O \otimes H_I) \Delta W^T = \text{tr}(\Delta W H_I \Delta W^T H_O) \quad (15)$$

$$= \text{tr}(\Delta W(L_I + I) D_I (L_I + I)^T \Delta W^T (L_O + I) H_O (L_O + I)^T) \quad (16)$$

$$= \text{tr}(\eta D_I \eta^T D_O) = \text{tr}(\eta^T \eta (D_O \otimes D_I)) \quad (17)$$

Since

$$\eta = W^* + L_O^T \Delta W L_I + L_O^T \Delta W + \Delta W L_I - W \quad (18)$$

$$= W^* + L_O^T \Delta W L_I + L_O^T \Delta W + \Delta W L_I - \mathcal{Q}(W^* + L_O^T \Delta W L_I + L_O^T \Delta W + \Delta W L_I) \quad (19)$$

$$= \star - Q(\star) \quad (20)$$

and \mathcal{Q} operates independently on $g_x \times g_y$ -sized blocks, we have that $\text{tr}(\eta^T \eta (D_O \otimes D_I)) \leq g_x g_y \sigma^2 \text{tr}(D_O \otimes D_I) = g_x g_y \sigma^2 \text{tr}(D_O) \text{tr}(D_I)$. From Chee et al. [3], we have that

$$\text{tr}(D) \leq \frac{\mu}{k} \text{tr}(H^{1/2})^2 \quad (21)$$

for arbitrary p.d. $H \in \mathbb{R}^{k \times k}$, so

$$\text{tr}(D_O) \text{tr}(D_I) g_x g_y \sigma^2 \leq \frac{g_x g_y \mu_I^2 \mu_O^2}{mn} \text{tr}(H_I^{1/2})^2 \text{tr}(H_O^{1/2})^2 \sigma^2 \quad (22)$$

□

Theorem 1. Let $H_O \in \mathbb{R}^{m \times m}$ and $H_I \in \mathbb{R}^{n \times n}$ be two positive definite matrices and let \mathcal{Q} perform nearest or stochastic rounding with $\mathbb{E}[(\mathcal{Q}(x) - x)^2] \leq \sigma^2$. Furthermore, let W be the output of Equation 10 with L_O and L_I from the LDL decompositions of H_O and H_I , respectively. Then,

$$\Delta W(H_O \otimes H_I) \Delta W^T \leq \text{tr}(D_I) \text{tr}(D_O) \sigma^2 \leq \frac{\mu_I^2 \mu_O^2}{mn} \text{tr}(H_I^{1/2})^2 \text{tr}(H_O^{1/2})^2 \sigma^2$$

where $\Delta W = W^* - W$ and μ_O, μ_I are the incoherences of H_O, H_I (Definition 2).

Proof. This follows from setting $g_x = g_y = 1$ in Theorem 3. □

Lemma 1. Let $A, B \in \mathbb{R}^{n \times n}$ be positive definite matrices and $x \in \mathbb{R}^n$ be a vector. Then, $\left| x^T \frac{A}{\|A\|} x - x^T \frac{B}{\|B\|} x \right| \leq \|x\|_F^2 \sqrt{2 - 2c}$ where $\frac{\langle A, B \rangle}{\|A\| \|B\|} = c$.

Proof.

$$\left| x^T \frac{A}{\|A\|} x - x^T \frac{B}{\|B\|} x \right| = \left| x^T \left(\frac{A}{\|A\|} - \frac{B}{\|B\|} \right) x \right| \quad (23)$$

$$\leq \left\| \frac{A}{\|A\|} - \frac{B}{\|B\|} \right\|_F \|x\|_F^2 \quad (24)$$

$$\leq \|x\|_F^2 \sqrt{2 - 2c} \quad (25)$$

□

Theorem 2. Let $H \in \mathbb{R}^{m \times n \times m \times n} = \nabla_{W*} L$ be the Hessian of a linear layer W with respect to the KL divergence to the original model outputs and let everything else be defined as in Theorem 1. Then,

$$\Delta W H \Delta W^T \leq \|H\| \left(\|\Delta W\|_F^2 \sqrt{2 - 2c} + \frac{\mu_I^2 \mu_O^2}{mn \|H_I\| \|H_O\|} \text{tr}(H_I^{1/2})^2 \text{tr}(H_O^{1/2})^2 \sigma^2 \right)$$

where $c = \frac{\langle H, H_O \otimes H_I \rangle}{\|H\| \|H_O\| \|H_I\|}$ is the cosine similarity between H and $H_O \otimes H_I$.

Proof. From Lemma 1, we have that

$$\left| \frac{\Delta W H \Delta W^T}{\|H\|} - \frac{\Delta W (H_O \otimes H_I) \Delta W^T}{\|H_O\| \|H_I\|} \right| \leq \|\Delta W\|_F^2 \sqrt{2 - 2c}. \quad (26)$$

Then,

$$\Delta W H \Delta W^T \leq \|H\| \left(\|\Delta W\|_F^2 \sqrt{2 - 2c} + \frac{\Delta W (H_O \otimes H_I) \Delta W^T}{\|H_O\| \|H_I\|} \right) \quad (27)$$

$$\Delta W H \Delta W^T \leq \|H\| \left(\|\Delta W\|_F^2 \sqrt{2 - 2c} + \frac{\mu_I^2 \mu_O^2}{mn \|H_I\| \|H_O\|} \text{tr}(H_I^{1/2})^2 \text{tr}(H_O^{1/2})^2 \sigma^2 \right). \quad (28)$$

□

A.6 Modified Pytorch Backward Pass to Compute Sketch A

```
class LinearNoBias(torch.autograd.Function):
    @staticmethod
    @torch.amp.custom_fwd(device_type='cuda')
    def forward(ctx, input, weight, mode, parent_class):
        ctx.save_for_backward(input, weight)
        ctx.mode = mode
        ctx.parent_class = parent_class

        return input @ weight.T

    @staticmethod
    @torch.amp.custom_bwd(device_type='cuda')
    def backward(ctx, grad_output):
        it, reset, div = ctx.mode
        is_buffer = local_rank == ctx.parent_class.buffer_dev

        input, weight = ctx.saved_tensors
        ws = weight.shape
        grad_input = grad_output @ weight
        del weight

        if ctx.parent_class.collect_hess:
            grad_output = grad_output.reshape(-1, grad_output.shape[-1])
            input = input.reshape(-1, input.shape[-1])
            op_dtype = ctx.parent_class.op_dtype
            with torch.amp.autocast('cuda', enabled=False):
                grad_output = grad_output.float()
                input = input.float()
                bs = input.shape[0]
                if it == 0:
                    del grad_output
                    if reset and is_buffer:
                        ctx.parent_class.hin.mul_(0)

                in_hess = sym_to_flat(input.T @ input) / ctx.parent_class.scale
                del input
                torch.distributed.reduce(in_hess, ctx.parent_class.buffer_dev, op=ReduceOp.AVG)

            if is_buffer:
                ctx.parent_class.hin.add_(in_hess.to(ctx.parent_class.hin.device).to(op_dtype))
                ctx.parent_class.ct += bs / ctx.parent_class.scale
                if div:
                    ctx.parent_class.hin.div_(ctx.parent_class.ct)
                ctx.parent_class.ct = 0

            del in_hess
            torch.cuda.empty_cache()
        else:
            if it % 2 == 0:
                if reset and is_buffer:
                    ctx.parent_class.hin.mul_(0)

                if not is_buffer:
                    out_hess = torch.zeros(ctx.parent_class.out_features * (ctx.parent_class.out_features + 1)//2, dtype=op_dtype, device=local_rank)
                else:
                    out_hess = ctx.parent_class.hout.to(local_rank)

                torch.distributed.broadcast(out_hess, ctx.parent_class.buffer_dev)
                out_hess = flat_to_sym(out_hess, ws[0]).float()
                in_hess = input.T @ (input * ((grad_output @ out_hess) * grad_output).sum(dim=-1, keepdims=True) / out_hess.norm()**2)
                del input, grad_output, out_hess
                in_hess = sym_to_flat(in_hess) / ctx.parent_class.scale
                torch.distributed.reduce(in_hess, ctx.parent_class.buffer_dev, op=ReduceOp.AVG)
                if is_buffer:
                    ctx.parent_class.hin.add_(in_hess.to(ctx.parent_class.hin.device).to(op_dtype))
```

```

        ctx.parent_class.ct += bs / ctx.parent_class.scale
        if div:
            ctx.parent_class.hin.div_(ctx.parent_class.ct)
            ctx.parent_class.ct = 0

        del in_hess
    else:
        if reset and is_buffer:
            ctx.parent_class.hout.mul_(0)

        if not is_buffer:
            in_hess = torch.zeros(ctx.parent_class.in_features * (ctx.parent_class.
in_features + 1)//2, dtype=op_dtype, device=local_rank)
        else:
            in_hess = ctx.parent_class.hin.to(local_rank)
            torch.distributed.broadcast(in_hess, ctx.parent_class.buffer_dev)
            in_hess = flat_to_sym(in_hess, ws[1]).float()
            out_hess = grad_output.T @ (grad_output * ((input @ in_hess) * input).sum(dim
=-1, keepdims=True)) / in_hess.norm()**2
            del input, grad_output, in_hess
            out_hess = sym_to_flat(out_hess) / ctx.parent_class.scale
            torch.distributed.reduce(out_hess, ctx.parent_class.buffer_dev, op=ReduceOp.AVG
)
        if is_buffer:
            ctx.parent_class.hout.add_(out_hess.to(ctx.parent_class.hout.device).to(
op_dtype))
            ctx.parent_class.ct += bs / ctx.parent_class.scale
        if div:
            ctx.parent_class.hout.div_(ctx.parent_class.ct)
            ctx.parent_class.ct = 0

        del out_hess

    torch.cuda.empty_cache()
    return grad_input.to(local_rank), None, None, None

```

A.7 Modified Backward Pass to Compute Sketch B

```

class LinearNoBias(torch.autograd.Function):
    @staticmethod
    @torch.amp.custom_fwd(device_type='cuda')
    def forward(ctx, input, weight, mode, parent_class):
        ctx.save_for_backward(input, weight)
        ctx.mode = mode
        ctx.parent_class = parent_class

        return input @ weight.T

    @staticmethod
    @torch.amp.custom_bwd(device_type='cuda')
    def backward(ctx, grad_output):
        it, reset, div = ctx.mode
        is_buffer = local_rank == ctx.parent_class.buffer_dev

        input, weight = ctx.saved_tensors
        ws = weight.shape
        grad_input = grad_output @ weight
        del weight

        if ctx.parent_class.collect_hess:
            op_dtype = ctx.parent_class.op_dtype
            bs = input.shape[0]
            with torch.amp.autocast('cuda', enabled=False):
                if it == 0:
                    if reset and is_buffer:
                        ctx.parent_class.hin.mul_(0)

                    grad_output = grad_output.float()
                    input = input.float()
                    in_hess = sym_to_flat(torch.einsum('btm,btn,bsm,bsk->nk', grad_output, input,
grad_output, input))
                    handle_in = torch.distributed.reduce(in_hess, ctx.parent_class.buffer_dev, op=
ReduceOp.AVG, async_op=True)
                    out_hess = sym_to_flat(torch.einsum('btm,btn,bsk,bsn->mk', grad_output, input,
grad_output, input))
                    handle_out = torch.distributed.reduce(out_hess, ctx.parent_class.buffer_dev, op=
ReduceOp.AVG, async_op=True)
                    del grad_output, input
                    handle_in.wait()
                    handle_out.wait()

                if is_buffer:
                    ctx.parent_class.hin.add_(in_hess.to(ctx.parent_class.hin.device).to(op_dtype))
                    ctx.parent_class.hout.add_(out_hess.to(ctx.parent_class.hout.device).to(
op_dtype))
                    ctx.parent_class.ct += bs
                if div:
                    ctx.parent_class.hin.div_(ctx.parent_class.ct)
                    ctx.parent_class.hout.div_(ctx.parent_class.ct)
                    ctx.parent_class.ct = 0

```

Table 5: Full zeroshot accuracy results for Table 1. Higher is better

MODEL	ALGO.	QUANT.	0-SHOT ACC \uparrow				
			ARCC	ARCE	BOOLQ	HSWAG	PIQA
3.1 70B INST	BF16	56.40	75.34	62.20	61.51	82.92	
		QTIP 2	52.05	73.91	62.17	58.10	81.01
		LDLQ	56.06	75.88	62.23	61.00	82.70
	YAQA-A	QTIP 4	55.72	75.63	62.29	61.18	83.08
		QTIP 2	52.82	74.07	62.17	58.27	82.26
		QTIP 3	56.07	75.88	62.20	61.84	82.46
	YAQA-B	QTIP 4	56.06	75.42	62.17	61.11	82.75
		QTIP 2	54.44	73.44	62.17	59.24	81.66
		QTIP 3	55.72	74.33	62.17	60.91	83.08
	BF16	56.31	76.09	62.29	61.10	82.86	
3.1 8B INST		51.37	78.03	82.05	57.74	79.92	
LDLQ	QTIP 2	41.89	74.28	67.98	51.67	76.71	
	QTIP 3	50.34	77.61	82.05	56.57	79.87	
	QTIP 4	50.68	78.07	80.98	57.32	79.98	
YAQA-A	QTIP 2	45.39	73.91	70.34	52.59	78.07	
	QTIP 3	49.83	77.23	81.76	56.85	79.76	
	QTIP 4	50.34	78.32	82.45	57.35	79.65	
YAQA-B	QTIP 2	44.20	75.08	70.64	52.91	78.78	
	QTIP 3	51.02	77.86	81.04	57.24	79.38	
	QTIP 4	50.94	78.49	82.02	57.47	79.98	
3.2 3B INST	BF16	44.45	71.42	76.18	51.19	75.73	
		QTIP 2	32.00	58.50	69.42	45.57	72.91
		LDLQ	41.72	70.66	74.19	50.46	75.24
	YAQA-A	QTIP 4	43.52	71.80	75.93	51.03	76.22
		QTIP 2	38.65	66.46	66.76	45.98	73.61
		QTIP 3	42.15	69.70	74.92	50.04	75.73
	YAQA-B	QTIP 4	42.66	70.24	76.57	50.85	76.06
		QTIP 2	38.05	68.22	68.75	47.11	73.39
		QTIP 3	42.75	69.95	75.66	50.38	74.97
		QTIP 4	43.60	71.04	75.96	50.74	75.19
3.2 1B INST	BF16	32.85	57.24	66.09	44.74	73.01	
		QTIP 2	27.30	51.60	61.71	38.66	68.72
		LDLQ	29.44	54.42	65.47	43.31	71.82
	YAQA-A	QTIP 4	30.46	54.76	65.84	43.70	72.58
		QTIP 2	27.59	51.55	62.84	39.28	68.86
		QTIP 3	32.17	56.02	65.47	43.51	72.14
	YAQA-B	QTIP 4	32.51	56.86	64.37	44.33	72.80
		QTIP 2	27.47	54.46	62.51	39.89	70.18
		QTIP 3	31.31	56.44	62.60	43.20	73.50
		QTIP 4	31.48	55.18	64.86	43.42	74.27

```

    del in_hess, out_hess
    torch.cuda.empty_cache()

    torch.cuda.empty_cache()
    return grad_input.to(local_rank), None, None, None

```

Table 6: Results without incoherence processing. All results are without finetuning and use an INT4 quantizer with a 16-bit groupwise scale shared across 32 contiguous elements (4.5 bits per weight amortized).

ALGO.	$D_{KL} \downarrow$		PPL \downarrow		0-SHOT ACC \uparrow				
	W2	W2	C4	AVG	ARCC	ARCE	BOOLQ	HSWAG	PiQA
BF16	0	6.50	8.02	69.82	51.37	78.03	82.05	57.74	79.92
LDLQ	0.033	6.75	8.21	68.35	49.74	77.36	78.35	56.83	79.49
YAQA-A	0.025	6.67	8.17	69.36	49.74	77.65	81.62	57.16	80.63
YAQA-B	0.021	6.65	8.15	68.95	50.68	78.20	79.72	57.06	79.11

A.8 Additional Results

Table 5 contains full zeroshot results from the “no finetuning” table in the main body. Table 6 shows an experiment without incoherence processing. All quantized models in this table use an INT4 quantizer with a 16 bit groupwise absmax scale shared across 32 contiguous elements, giving an effective 4.5 bits per weight. We used $g_x = 1$ and $g_y = 32$ for all methods. Even with out incoherence processing, YAQA outperforms LDLQ.